MULTI-DIMENSIONAL BIOMEDICAL IMAGE DE-NOISING USING HAAR TRANSFORM

Eva Hostalkova, Oldrich Vysata, Ales Prochazka

Institute of Chemical Technology in Prague, Department of Computing and Control Engineering
Technicka Street 5, 166 28 Prague 6, Czech Republic
Email: Eva.Hostalkova@vscht.cz, Vysata@neurol.cz, A.Prochazka@ieee.org
Phone: +420 220 444 198, Web: dsp.vscht.cz

ABSTRACT

Image de-noising and enhancement form fundamental problems in many engineering and biomedical applications. The paper is devoted to the study of the multi-resolution approach to this problem employing the Haar wavelet transform. The transform is applied to volumetric magnetic resonance (MR) image sets corrupted with additional noise. The resulting coefficients are thresholded and exploited for subsequent reconstruction. The Haar transform is carried out through both the two-dimensional approach applied individually to each image layer, and the three-dimensional technique performed on the image volume as a whole. In noise reduction, the latter approach profits from similarities between neighbouring image layers and shows a considerable improvement over the former method. Results are presented both in the numerical form and using three-dimensional visualization tools.

Index Terms— Wavelet transform, image decomposition and reconstruction, Haar transform, de-noising, biomedical image processing

1. INTRODUCTION

Fundamental problems encountered in the digital processing of both one-dimensional and multi-dimensional signals include rejection of their undesirable parts [1, 2],feature extraction, classification and restoration of their missing or corrupted components. Multi-resolution approach related to wavelet transform [3, 4, 5] is used in many cases to simplify these processes and to improve their robustness. Image resolution enhancement [6, 7] and volumetric reconstruction [8, 9] form further problems related to these topics.

Biomedical image processing form an extensive area based upon theoretical principles of multi-dimensional processing methods. Related problems include multirate analysis, processing and coding of biomedical images [10, 11].

The paper is devoted to the use of the wavelet transform and multi-resolution decomposition of biomedical image volumes to improve results of the de-noising process applied separately to every image layer of the body. In the initial part of the paper, the Haar transform computation algorithm is proposed starting with 1-D signal and proceeding to 2-D images and 3-D image sets.

The proposed method is applied to multi-layer magnetic resonance (MR) biomedical images. An example of the biomedical structure studied further is presented in Fig. 1. After noise addition, these multi-layer images are processed by both 2-D and 3-D Haar transform involving the coefficients thresholding procedure. Specific topics of the use of the wavelet functions in magnetic resonance imaging are studied by many authors nowadays [12, 13].

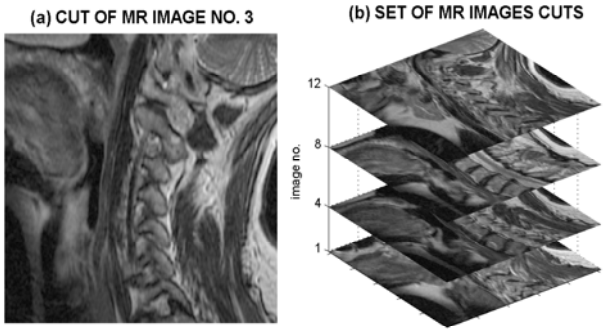

Fig. 1. Real data standing for **(a)** a selected spinal MR image and **(b)** four chosen slices of these MR data set 3

2. HAAR TRANSFORM IN SIGNAL ANALYSIS

The Haar transform stands for the simplest algorithm enabling signal or image compression [14].

Let us have a signal $\{x(n)\}_{n=1}^{N}$. Each couple of its subsequent values $\{x(n), x(n+1)\}$ for $n = 1, 3, \cdots, N$ can then be decomposed into two values

$$\begin{pmatrix} X_n \\ X_{n+1} \end{pmatrix} = \mathbf{T} \begin{pmatrix} x_n \\ x_{n+1} \end{pmatrix} \tag{1}$$

where

$$\mathbf{T} = \frac{1}{\sqrt{2}} \begin{pmatrix} 1 & 1 \\ 1 & -1 \end{pmatrix} \tag{2}$$

Thanks to Research grant No. MSM 6046137306

Resulting sequence $\{X_1, X_3, \cdots, X_{N-1}\}$ defines the low-pass decomposition values with its length halved in comparison with the original sequence. The complementary high-pass sequence is composed by values $\{X_2, X_4, \cdots, X_N\}$ in the same way.

A similar principle can be applied to the analysis of an image $[g(n,m)]_{N,M}$ taking into account that a one-dimensional signal can be considered as a special case of an image having only one column. The elementary decomposition element is a 2 x 2 matrix

$$\begin{pmatrix} g_{n,m} & g_{n,m+1} \\ g_{n+1,m} & g_{n+1,m+1} \end{pmatrix} \tag{3}$$

in this case for $n = 1, 3, \cdots, N-1$ and $m = 1, 3, \cdots, M-1$. Each such submatrix is decomposed column-wise at first

$$\begin{pmatrix} G1_{n,m} & G1_{n,m+1} \\ G1_{n+1,m} & G1_{n+1,m+1} \end{pmatrix} = \mathbf{T} \begin{pmatrix} g_{n,m} & g_{n,m+1} \\ g_{n+1,m} & g_{n+1,m+1} \end{pmatrix} \tag{4}$$

and then row-wise using relation

$$\begin{pmatrix} G_{n,m} & G_{n,m+1} \\ G_{n+1,m} & G_{n+1,m+1} \end{pmatrix} = \begin{pmatrix} G1_{n,m} & G1_{n,m+1} \\ G1_{n+1,m} & G1_{n+1,m+1} \end{pmatrix} \mathbf{T}^T \tag{5}$$

In this manner, the first level of the decomposition procedure is complete. The resulting matrix elements may be rearranged to define four submatrices. The low/low-pass submatrix is defined hereby

$$\begin{pmatrix} G_{1,1} & G_{1,3} & \cdots & G_{1,M-1} \\ G_{3,1} & G_{3,3} & \cdots & G_{3,M-1} \\ & & \cdots & \\ G_{N-1,1} & G_{N-1,3} & \cdots & G_{N-1,M-1} \end{pmatrix} \tag{6}$$

This matrix having the half number of rows and columns comparing to the original one can be used for the next level of decomposition. Results of 2-D Haar decomposition into the first level for a spinal MR image are presented in Fig. 2.

In a similar way, it is possible to decompose the body consisting of layers of images. The mathematical principle [15, 14] is based upon the generalization of the previous method adding another axis in the layer direction. In other words, pixels of the outcome of 2-D transform of all image layers, which have the corresponding x,y-location, are decomposed as well as 1-D signals. The 3-D decomposition of a spinal MR image volume using the Haar decomposition matrix is shown in Fig. 3. Further possibilities include application of complex wavelet functions [16].

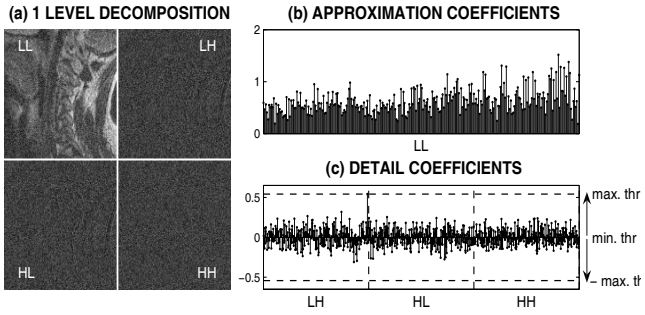

Fig. 2. Decomposition of the MR image image with additional random noise using Haar transform presenting **(a)** results of one level image decomposition, **(b)** approximation decomposition coefficients, and **(c)** detail decomposition coefficients

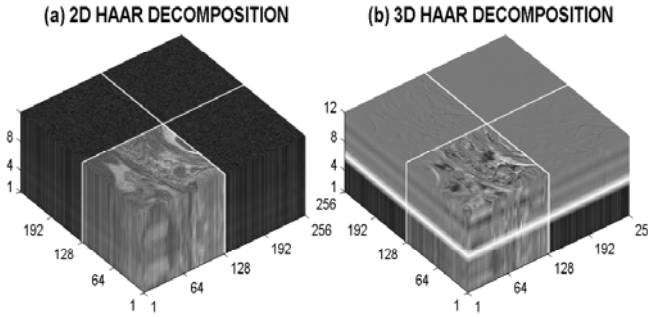

Fig. 3. Decomposition of the set of MR images presenting **(a)** 2-D slice-by-slice Haar wavelet decomposition **(b)** 3-D volumetric Haar wavelet decomposition

3. OPTIMAL THRESHOLD SELECTION FOR IMAGE DE-NOISING

Image de-nosing can by achieved by appropriate thresholding of wavelet coefficients. In the case of soft-thresholding it is possible to evaluate new coefficients $\overline{c}(k)$ using original coefficients $c(k)$ for a chosen threshold value δ by relation

$$\overline{c}(k) = \begin{cases} \text{sign } c(k)\ (|c(k)| - \delta) & \text{if } |c(k)| > \delta \\ 0 & \text{if } |c(k)| \leq \delta \end{cases} \tag{7}$$

This approach can be exploited both for signals and images using different methods of threshold level estimation. Fig.4(a) presents results of a selected numerical experiment showing the dependence of the MSE for a chosen image de-noising with respect to the threshold limits chosen between the minimum and maximum values of the detail decomposition coefficients. In this way, the optimal value of threshold level is found for each image layer. In the case of 3-D decomposition, a single threshold value is estimated for the whole volume. Results of the 2-D de-nosing of the selected MR image using global thresholding and the optimal threshold value are presented in Figs 4(b), (c) and (d).

4. MULTIDIMENSIONAL OBJECT DE-NOISING

Signal de-noising procedure applied in two dimensions can be further generalized to three dimensions. The problem is to find to which extend space information can improve de-noising results and enhancement of individual images.

The following study is devoted to the problem of noise rejection in real MR images. Table 1 summarizes specifications of MR data sets used for this study presenting different biomedical structures. Fig. 1 shows parts of the set 3 composed of 12 layers with resolution of 256 x 256 pixels.

Table 1. MRI DATA SETS SPECIFICATIONS

MRI Set	*Data Type*	*Pixel Spacing [mm]*	*Slice Spacing [mm]*	*Block Size*
1	Spine - Sagittal	0.4687	4	512x512x12
2	Spine - Axial	0.3906	4	512x512x26
3	Cut of Set 1	0.4687	4	256x256x12
4	Cut of Set 2	0.3906	4	256x256x26
5	Brain - Axial	0.4688	1	256x256x12

Fig. 5 shows results achieved for selected sets of MR images. The additional random noise was rejected using both 2-D and 3-D Haar decomposition and thresholding of the resulting coefficients.

Numerical results are summarized in Table 2 for five selected MR sets. The mean square error (MSE) between the original image volume and the de-noised one is normalised to

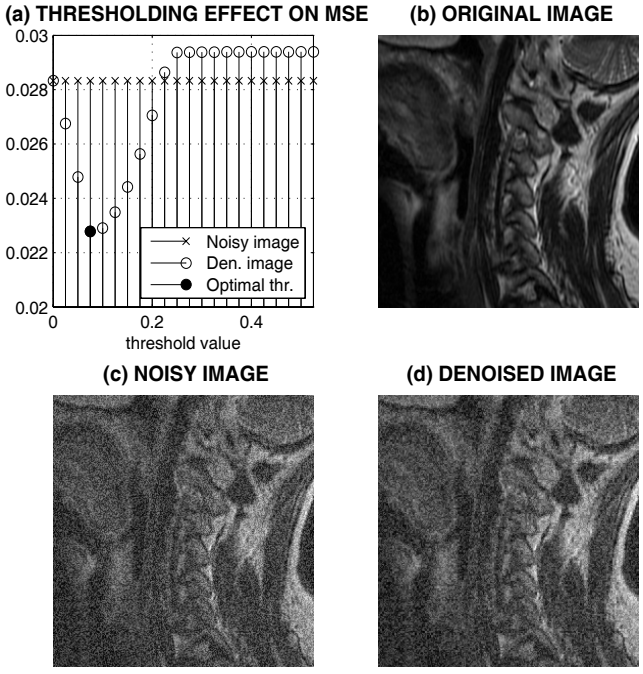

Fig. 4. Processing of the spinal MR image number 3 presenting **(a)** the effect of threshold selection on the mean square error (MSE) value, **(b)** original image, **(c)** image with additional random noise, and **(d)** de-noised image using the optimal threshold value

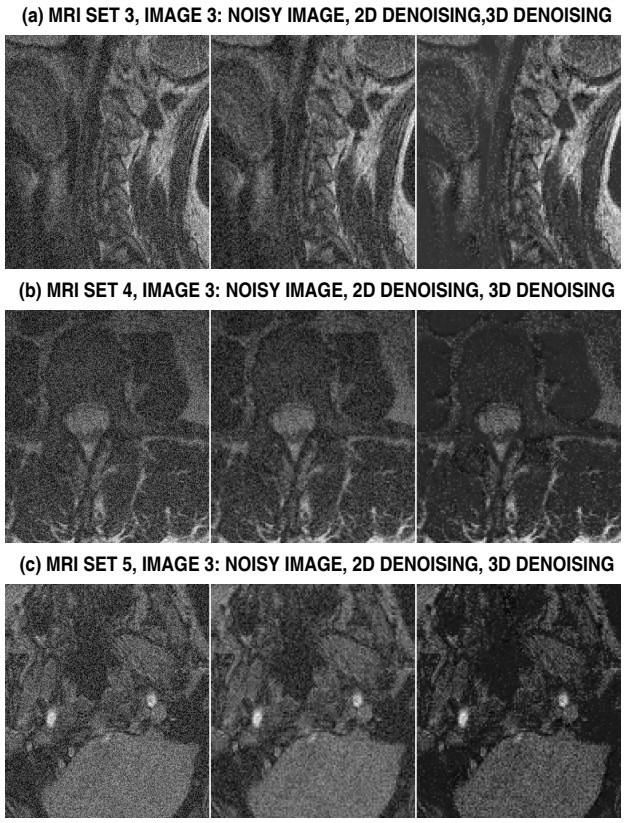

Fig. 5. MR image de-noising by thresholding the 2D and 3D Haar coefficients for **(a)** image number 3 of MRI set 3 (sagittal spine), **(c)** image number 3 of MRI set 4 (axial spine), and **(c)** image number 3 of MRI set 5 (axial brain)

the number of pixels in each image set. For each of the five sets of data, we carried out ten 2-D and ten 3-D de-noising experiments, each time with a different random noise component. Table 2 displays the average MSE, its variance and its percentage improvement attained by de-noising. Both numerical results and their visualization presented in Fig. 5 verify that the 3-D approach to image processing can highly improve results achieved by the de-noising of individual layers.

Another set of numerical experiment have been done with a specific noise related to the random one with its low frequency spectral components removed in the frequency domain. Accomplishing the same set of experiments with this high frequency band noise, much better results were achieved for both de-noising methods. The overall average improvement was 74.2% for the 2-D de-noising and 87.2% for the 3-D de-noising. In this case, the advantages of the volumetric approach were not revealed in the full scale.

However, in the case of random noise, the layer-by-layer technique proves insufficient in comparison with the volumetric one. The percentage decrease of the random noise components summarised in Table 2 points out the substantial effect of the 3-D approach. While the overall average improvement

was 25.5% for the single layer processing, it was possible to achieve the improvement of 65.0% by the 3-D de-noising approach.

Table 2. COMPARISON OF THE DE-NOISING RESULTS FOR THE 2-D AND 3-D HAAR TRANSFORM

Method / Measure		*MRI Set*				
		1	*2*	*3*	*4*	*5*
2D	*MSE [E-02]*	2.69	2.27	1.81	1.77	1.97
	Variance [E-07]	8.25	3.39	14.9	2.68	13.0
	Improvement [%]	17.9	24.0	26.8	33.4	24.9
3D	*MSE [E-02]*	1.56	0.91	1.14	0.72	0.62
	Variance [E-07]	13.8	1.10	5.40	0.71	1.91
	Improvement [%]	52.5	69.6	53.9	73.0	76.2

5. CONCLUSION

It is possible to summarize that the 3-D image de-noising can significantly improve results achieved in the case of processing of individual images. Results presented in Table 2 summarize numerical experiments for real MR biomedical bodies using the Haar volumeric decomposition enabling also very simple reconstruction of the three-dimensional body.

Our further studies will be devoted to the application of specific wavelet functions for volumetric enhancement of biomedical structures. The purpose of such a study is in the detection of image components and in visualization of general slices of the 3-D structures.

6. REFERENCES

[1] D. E. Newland, *An Introduction to Random Vibrations, Spectral and Wavelet Analysis*, Longman Scientific & Technical, Essex, U.K., third edition, 1994.

[2] Saeed Vaseghi, *Advanced Digital Signal Processing and Noise Reduction*, John Wiley & Sons, West Sussex, U.K., third edition, 2006.

[3] N. Kingsbury, "Complex Wavelets for Shift Invariant Analysis and Filtering of Signals," *Journal of Applied and Computational Harmonic Analysis*, vol. 10, no. 3, pp. 234–253, May 2001.

[4] S. Li and J. Shawe-Taylor, "Comparison and Fusion of Multiresolution Features for Texture Classification," *Pattern Recogn. Lett.*, vol. 25, 2004.

[5] M. Weeks and M. A. Bayoumi, "Three-Dimensional Discrete Wavelet Transform Architectures," *IEEE Transactions on Signal Processing*, vol. 50, no. 8, pp. 2050 – 2063, 2002.

[6] J. Ptáček, I. Šindelářová, A. Procházka, and J. Smith, "Wavelet Transforms In Signal And Image Resolution Enhancement," in *International Conference Algoritmy 2002, Podbanske*. 2002, STU.

[7] A. Procházka and J. Ptáček, "Wavelet Transform Application in Biomedical Image Recovery and Enhancement," in *The 8th Multi-Conference Systemics, Cybernetics and Informatic, Orlando, USA*. 2004, vol. 6, pp. 82–87, IEEE.

[8] Xiaohui Yuan and G. Chi-Fishman, "Volumetric Tongue Reconstruction by Fusing Bidirectional MR Images," in *3rd IEEE International Symposium on Biomedical Imaging: Macro to Nano*. 2006, pp. 1352 – 1355, IEEE.

[9] V. Thirumalai and R. Kanhirodan, "Wavelet Transform Codec for Fast Retrieval of Slices of 3D Objects," in *Proceedings of the IEEE Instrumentation and Measurement Technology Conference, IMTC 2005*. 2005, vol. 2, pp. 1251 – 1254, IEEE.

[10] G. Menegaz and L. Grewe and J. P. Thiran, "Multirate Coding of 3D Medical Data," in *Proceedings of the 2000 International Conference on Image Processing*. 2000, vol. 3, pp. 656 – 659, IEEE.

[11] J. Wang and H. K. Huang, "Medical Image Compression by Using Three-Dimensional Wavelet Transform," *IEEE Transactions on Medical Imaging*, vol. 15, no. 4, pp. 547 – 554, 1996.

[12] M. Breakspear, M. Brammer, E. Bullmore, P. Das, and L. Williams, "Spatiotemporal Wavelet Resampling for Functional Neuroimaging Data," *Human Brain Mapping*, vol. 23, no. 1, pp. 1–25, 2004.

[13] E. Bullmore, J. Fadili, V. Maxim, L. Sendur, J. Suckling B. Whitcher, M. Brammer, and M. Breakspear, "Wavelets and Functional Magnetic Resonance Imaging of the Human Brain," *NeuroImage*, vol. 23, no. Sup 1, pp. 234–249, 2004.

[14] D. Montgomery and F. Murtagh and A. Amira, "A Wavelet Based 3D Image Compression System," in *Proceedings of the Seventh International Symposium on Signal Processing and Its Applications*. 2003, vol. 1, pp. 65 – 68, IEEE.

[15] C. Zhang and H. X. Zheng and D. B. Ge, "3-D Wavelet-Based Multiresolution Analysis," in *Proceedings of the 5th International Symposium on Antennas, Propagation and EM Theory*. 2000, pp. 301 – 304, IEEE.

[16] N. Kingsbury and A. Zymnis and A. Pena, "DT-MRI Data Visualisation Using the Dual Tree Complex Wavelet Transform," in *3rd IEEE International Symposium on Biomedical Imaging: Macro to Nano*. 2004, pp. 328 – 331, IEEE.